RSC Advances

ROYAL SOCIETY OF CHEMISTRY

www.rsc.org/advances

Porous polyethersulfone hollow fiber membrane in gas humidification process

Gh. Bakeri [a]*, S. Naeimifard [a], T. Matsuura [b,c], A.F. Ismail [b]*

[a] Advanced Membrane and Biotechnology Research Center, Faculty of Chemical Engineering, Babol Noshirvani University of Technology, Babol, Iran

[b] Advanced Membrane Technology Research Centre (AMTEC), Universiti Teknologi Malaysia, 81310 Skudai, Johor, Malaysia

[c] Industrial Membrane Research Institute, Department of Chemical and Biological Engineering, University of Ottawa, Ottawa, ON, K1N 6N5, Canada

*Corresponding authors: bakeri@nit.ac.ir; afauzi@utm.my

Tel: +98 912 526 5739; Fax: +98 11 323 34 204

Abstract

Porous polyethersulfone hollow fiber membrane was fabricated via dry-wet phase inversion process. The membrane was characterized by measuring pore size, porosity and LEPw. Scanning electron microscopy (SEM) revealed the presence of finger-like macrovoids in the cross-section of the membrane, which contributed to the reduction of tortuosity.

The fabricated membrane was further applied in gas humidification. It was found that the water flux was increased by an increase in the gas and liquid flow rates and temperature but reduced by an increase in gas pressure. The water flux of fabricated membrane exhibited gas humidification performance superior to a commercial humidifier, e.g. it has 380% higher water flux than Perma Pure®[1] model PH-60T-24SS at T_{liquid} = 40 °C.

Keywords: humidification process, membrane contactor, porous polyethersulfone hollow fiber membrane, relative humidity, water flux

1. Introduction

Gas humidification process is a major part of various technologies such as fuel cell technology, environmental air/gas humidification, reactant gas humidification and respiratory gas humidification in which the water content of the dry gas(es) should be increased to a specified value, e.g. in proton exchange membrane fuel cell (PEMFC) technology the feed gases (H_2 and O_2) should be humidified with water vapor to prevent drying of membrane otherwise the membrane shows higher ionic resistance and the efficiency of PEMFC reduces; or in crop storage, humidification of harvested crop increases the shelf life of the products.

Different methods have been proposed for humidification process such as bubble column [1] in which gas is bubbled in water, spray column [2] in which water is sprayed in gas stream etc., all of which suffer from operational difficulties such as low water transfer rate, high operating cost, low efficiency, mist entrainment etc. Furthermore, these processes need large equipment and a high capital investment.

One alternative for gas humidification is the application of membrane technology which offers the advantages [3] such as low operating cost, high modularity and easy control of humidity. In particular, compactness with high water transfer rate seems the most important in fuel cell applications.

In membrane humidification process, liquid water flows on one side of a membrane, dissolves in the membrane and diffuses to the other side of the membrane, the water is evaporated and carried away by a gas stream. The process, also known as adiabatic humidification, is hence based on the solution-diffusion mechanism where a dense membrane such as Nafion

membrane is used. The drawback of the process is a very slow mass transfer, requiring high surface area and capital cost. As well, Nafion membrane is very expensive.

In a membrane contactor a porous membrane is used. In contrast to the dense membrane, in a porous membrane water is in contact with one side of a membrane, evaporates at the mouth of membrane pores, diffuses through the pores and the gas side boundary layer, and finally reaches the bulk of the gas stream. As the membrane is porous, water molecules move through the gas filled pores of the membrane fast, facilitating the transport of water. Therefore, membrane contactor based humidifiers are expected to show higher water transfer rate than Nafion membrane based humidifiers.

The application of a composite membrane, which consists of hydrophilic poly(N,N-dimethylaminoethyl methacrylate) (PDMAEMA) as the active layer (in contact with water) and polyacrylonitrile (PAN) as the substrate (in contact with gas), in humidification process was studied by Du et al. [4]. The water flux increased with gas flow rate and temperature of water but the humidity decreased with the gas flow rate.

Polytetrafluoroethylene (PTFE) porous flat sheet membrane with a pore size of 0.3 μm was used in gas humidification system for polymer electrolyte fuel cell (PEMFC) [5]. It was reported that the performance of the system was comparable with the bubble humidifier. The relative humidity of the exit gas from humidifier decreased rapidly with increasing the gas flow rate whereas it was nearly independent of the liquid flow rate. In addition, the relative humidity of the exit gas increased from 65% to 90% when the water temperature increased from 30 ^{o}C to 50 ^{o}C.

A quasi-counter flow parallel-plate membrane contactor (QCFPMC) was used by Yang et al. [6] for air humidification process. They used flat sheet PVDF and PTFE porous membranes in a contactor. In their study they defined the effectiveness as:

$$e = \frac{w_{out} - w_{in}}{w_s - w_{in}} \quad (1)$$

where w_s, w_{in} and w_{out} are the humidity ratios (in terms of kg water/kg dry gas) of the saturated state, inlet and outlet states, respectively. They found that the effectiveness decreased as the gas flow rate increased, improved as the liquid flow rate and liquid temperature increased and decreased as the membrane pore size increased. They concluded that the PTFE membrane showed higher performance than the PVDF membrane.

The application of flat sheet porous (polysulfone UF membrane) and nonporous membranes (Nafion 112, Nafion 115 and Nafion 117) in gas humidification process was investigated by Park et al. [3] to know the effect of flow rate and temperature. The porous membrane showed better results than the Nafion membranes.

There are two mass transfer resistances in the gas humidification by a porous membrane. One is the mass transfer resistance of the membrane that depends on the membrane properties such as pore size and pore size distribution, porosity and surface hydrophobicity, as the penetration of water into membrane pores reduces the performance of the contactor. The other is at the boundary layer in the gas phase that depends on the gas flow regime in the contactor module, i.e. the higher the turbulency in the gas phase the lower the mass transfer resistance. This aspect is controlled by the gas flow rate and the geometry of contactor module.

In the liquid phase, as the liquid is generally pure water, there is no mass transfer resistance [7]. But as the liquid evaporates at the membrane-liquid interface, the temperature of liquid at the interface drops, causing further decrease in vapor transport. The temperature at the interface depends on the liquid side flow regime and temperature.

The objective of this research is the application of porous hollow fiber PES membrane in gas humidification process. To the best of our knowledge, this system has not yet been investigated until now. The membrane was fabricated via dry-wet phase inversion process where water as a nonsolvent additive was added to the spinning solution to promote the phase inversion process. The fabricated membrane was characterized by different techniques and used in a membrane contactor to humidify dry nitrogen gas. The effects of gas and liquid flow rates, water temperature and the gas pressure on the water flux and humidity of the exit gas were studied.

2. Experimental

2.1. Materials

Polyethersulfone (PES) purchased from Arkema Inc. was dried at 70 ^{o}C overnight before use. N-Methyl-2-pyrrolidinone (NMP) [CAS No. 872-50-4] with a purity of 99.5 wt% purchased from Merck was used as solvent without further purification. Distilled water was used as nonsolvent additive to the polymer solution. Helium gas with a purity more than 99.5 vol% was used for gas permeation test and nitrogen gas with a purity more than 99 vol% was used for gas humidification tests.

2.2. Dope preparation

Predetermined amount of PES polymer was dissolved in NMP to make 25 wt% solution which was further mixed with NMP and distilled water to prepare the spinning dope. The composition of the spinning dope is given in Table 1. The viscosity of the polymer solution was measured using viscometer EW-98965-40, Cole Parmer, USA.

Table 1: Compositions of spinning solution.

PES (wt%)	Water/NMP	Solvent (wt%)	Solution viscosity (centipoise)
15	0.05	85	216.8

2.3. Preparation of hollow fibers

Spinning of hollow fibers by the Dry-wet spinning method is described elsewhere in detail [8]; briefly the polymer solution and bore fluid were extruded from the annulus and the tube of a tube-in-orifice spinneret, respectively, at constant flow rates. After traveling through the air gap (1 cm), the fibers went into a water bath of ambient temperature, where the nascent fibers was coagulated. After spinning, the fibers were kept immersed in water for several days to remove the residual solvent and then dried naturally at room temperature while being hung vertically. The spinning conditions are given in Table 2.

Table 2: Hollow fiber spinning conditions.

Air gap (cm)	1
Bore fluid	Distilled water
External coagulant	Tap water
Bore fluid temperature (^{o}C)	Room temperature
External coagulant temperature (^{o}C)	Room temperature

2.4. Hollow fiber module preparation and gas permeation test

The fibers were assembled in a module to conduct the gas permeation and liquid entry pressure of water (LEPw) tests. One end of fibers was closed with epoxy glue while the other

end was potted in stainless steel tubing. In gas permeation test, the permeated gas flows through the open end to the bubble flow meter while in liquid entry pressure of water test, water was sent to the lumen side of fiber through the open end.

As the membrane is porous, the pore size of the membrane has a critical effect on its performance; the larger the pores the more is the flux of water vapor through the membrane. But, on the other hand, the easier becomes the penetration of water into membrane pores, which leads to rapid reduction of the flux. Among many methods proposed to determine the membrane pore size, the gas permeation test seems one of the simplest, since it requires only the measurement of gas permeance at different pressures. The gas permeation system used in this work is shown schematically in Fig. 1, where helium gas is sent to the shell side of the module and the flow rate of the permeated gas through the lumen side of membrane is measured by a bubble flow meter. In gas permeation test it is assumed that the pores are cylindrical and straight and the flow of gas is under the combined Poiseuille and Knudsen flow regimes [9].

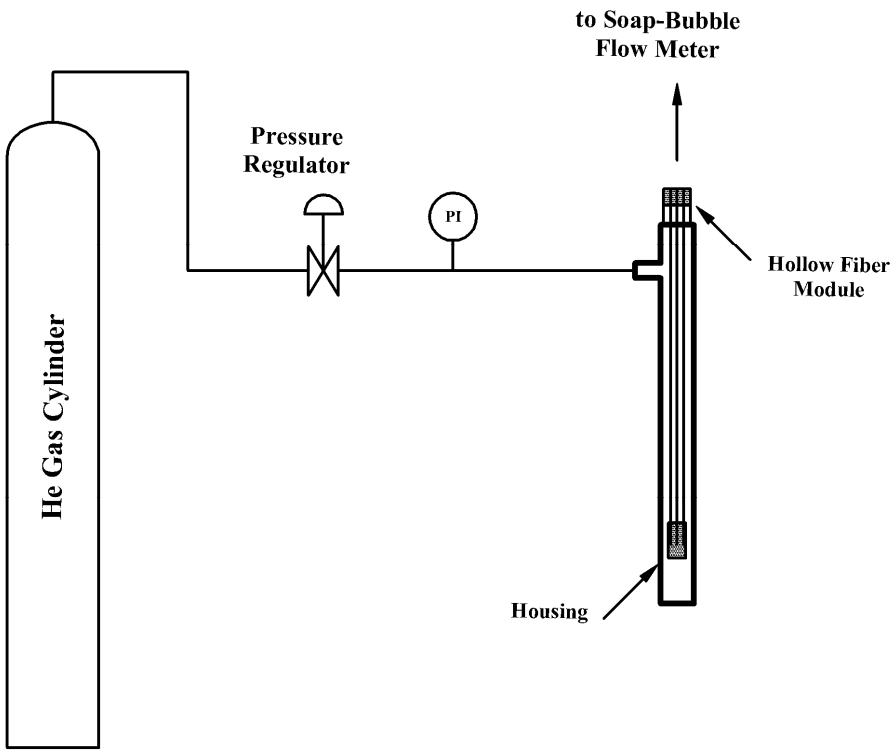

Fig. 1: Schematic of gas permeation test system.

Accordingly, the total gas permeance can be written as Eq. 2.

$$\overline{P} = P_P + P_K = \frac{2}{3}\left(\frac{8RT}{\pi M}\right)^{0.5}\frac{r_{P,m}}{RT}\frac{\xi}{L_P} + \frac{1}{8\mu}\frac{r_{P,m}^2}{RT}\frac{\xi}{L_P}\overline{p} \qquad (2)$$
$$\overline{P} = A + B\overline{p}$$

where P_K and P_P are the gas permeance (mol m^{-2} Pa^{-1} s^{-1}) under the Knudsen and Poiseuille flow regime, respectively, $\overline{P}$ is the total gas permeance (mol m^{-2} Pa^{-1} s^{-1}), T is the absolute temperature (K), $r_{P,m}$ is the mean pore radius (m), ξ is surface porosity ($\frac{A_P}{A_T}$ where A_P is the area of pores and A_T is total area of membrane), L_P is the effective pore length (m), R is the universal gas constant (8.314 J mol^{-1} K^{-1}), M is the molecular weight of gas (kg mol^{-1}), μ is the viscosity of gas (Pa. s) and $\overline{p}$ is the mean pressure (Pa) ($\frac{p_u + p_d}{2}$ where p_u is upstream

pressure and p_d is downstream pressure). Therefore, the plot of $\overline{P}$ versus $\overline{p}$ should be a straight line of which the slope and intercept of the line can be used in Eqs. 3-4 to calculate the mean pore size and effective surface porosity of membrane.

$$r_{P,m} = \frac{16}{3}\frac{B}{A}\left(\frac{8RT}{\pi M}\right)^{0.5}\mu \quad (3)$$

$$\frac{\xi}{L_P} = \frac{8\mu RTB}{r_{P,m}^2} \quad (4)$$

In this study, helium gas was used as the feed gas and the permeance was measured at various pressures that ranged from 1 to 3 barg.

2.5. Measurement of Liquid Entry Pressure of water (LEPw)

Liquid entry pressure is the minimum pressure required to let the liquid enter into membrane pores. It depends on the surface properties of membrane such as the pore size and the surface hydrophobicity. It also depends on the properties of liquid such as surface tension. When LEPw is too low, the membrane is more susceptible to the pore wetting.

The same module for gas permeation test was used to measure the LEPw. Five fibers were assembled in the module. Distilled water was supplied to the lumen side of the fibers and the pressure was slowly increased with a step size of 0.2 bar. The pressure at which the first water droplet appeared at the outer surface of membrane was reported as LEPw.

2.6. Membrane porosity and tortuosity

As the diffusion of water vapor takes place in the membrane pore, the membrane porosity should have a strong effect on the vapor flux. Hence the porosity is measured by the method

described elsewhere in detail [10]. Briefly, the weight and length of wet and dry hollow fibers were measured to obtain the membrane porosity (ε) through Eqs. 5-9.

$$F = \frac{dry\ membrane\ weight}{wet\ membrane\ weight} \quad (5)$$

$$S_l = \frac{wet\ membrane\ length - dry\ membrane\ length}{wet\ membrane\ length} \quad (6)$$

$$E = 1-(1-S_l)^3 \quad (7)$$

$$\rho_m = \frac{F}{(\frac{F}{\rho_P}+\frac{1-F}{\rho_{water}})(1-E)} \quad (8)$$

$$\varepsilon = \frac{\frac{1}{\rho_m}-\frac{1}{\rho_P}}{\frac{1}{\rho_m}} \quad (9)$$

where F is the mass fraction of polymer in the membrane, S_l is the longitudinal shrinkage of hollow fibers, E is the overall shrinkage of membrane during drying, ρ_m is the density of membrane, ρ_{water} is the density of water and ρ_P is polymer density which is 1.55 g cm^{-3} for PES.

The membrane tortuosity depends on the geometry of membrane pores; the higher the tortuosity the slower the mass transfer. Srisurichan et al. [11] proposed Eq. 10 to calculate the membrane tortuosity (τ) from the membrane porosity (ε).

$$\tau = \frac{(2-\varepsilon)^2}{\varepsilon} \quad (10)$$

2.7. Cloud point measurement

The thermodynamic stability of the spinning solution was evaluated by measuring the cloud point. Water was added as the coagulant drop-wise to the spinning solution with gentle mixing at room temperature until the solution could remain cloudy for a few hours. From the weight of the added coagulant, the composition at the cloud point was determined. The experiments were conducted at room temperature.

2.8. Scanning Electron Microscopy (SEM)

Scanning electron microscopy was used to observe the structure of membrane cross-section with a magnification of 400. The fiber was broken in liquid nitrogen and then platinum (Pt) sputtered.

2.9. Gas humidification test

The humidification system is presented schematically in Fig. 2. Both ends of hollow fiber membranes were potted in a stainless tubing (d_i = 1 cm) and cut after the epoxy resin was hardened to make them open. The module was insulated to prevent any heat transfer from/to environment. Water was pumped from the reservoir to the lumen side of the hollow fiber after being heated in a heat exchanger. The pressure of water was monitored by the pressure gauge while the liquid (water) flow rate was controlled by the valve at the exit of liquid.

Dry nitrogen gas flowed into the shell side of the hollow fiber module in a counter current mode. Gas flow rate was controlled by a mass flow controller (model: Aalborg DFC26) and the gas pressure by the valve at the gas exit. To prevent the bubbling of the gas into the liquid, the pressure of liquid was maintained 0.5 bar higher than gas.

The temperature and relative humidity (RH) of gas was measured at the contactor exit by humidity analyzer (model: Lutron LM-8000). The flux of water transferred to the gas stream was calculated through the temperature and relative humidity of the exit gas and the flow rate of dry N_2 gas.

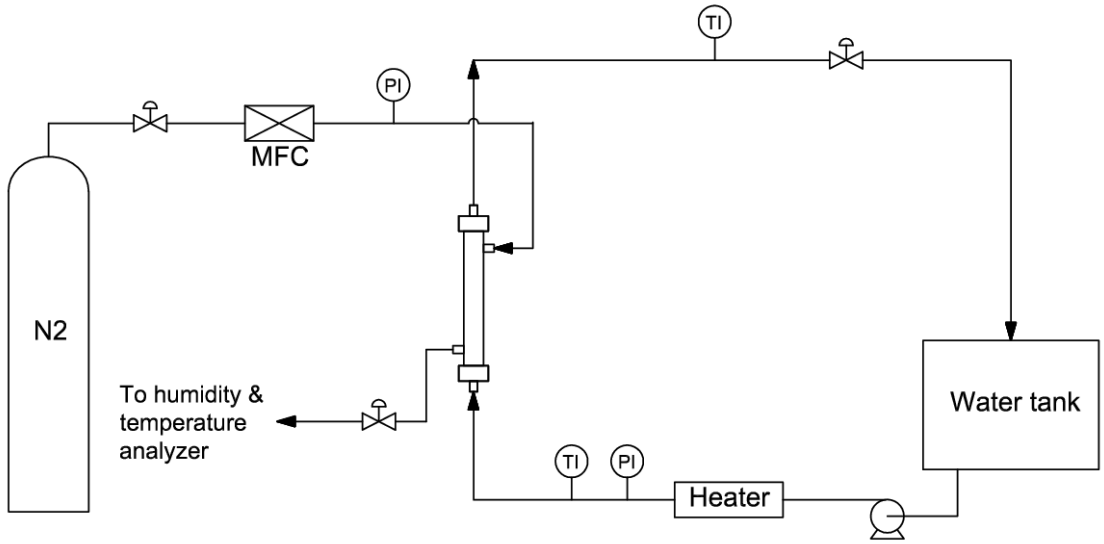

Fig. 2: Schematics of humidification system, TI: temperature indicator, PI: pressure indicator, MFC: mass flow controller.

The effects of liquid and gas flow rates, inlet liquid temperature and pressure of the inlet gas on the water vapor flux and relative humidity of exit gas were investigated. The operational parameters at which experiments were conducted are presented in Table 3.

Table 3: The range of investigated parameters in humidification process.

Parameter	Investigated value
Liquid temperature (^{o}C)	30, 45, 60, 75
Gas pressure (bar)	1, 3
Gas flow rate (standard liter per minute (SLPM))	1, 2, 3, 4, 5

3. Results and discussion

3.1. Membrane characterization test results

The fabricated membrane was characterized by different test methods and the results are presented in Table 4. The porosity of the membrane is high due to low polymer concentration which was found to be only 14% at the cloud point. The low viscosity of polymer solution also facilitated the intrusion of the coagulant during the phase inversion process [12]. The rapid phase inversion promotes the formation of fingerlike macrovoids [13,14], which increases the void fraction of membrane and reduces the membrane tortuosity.

Table 4: Membrane characterization tests results.

Mean pore size (nm)	653
Effective surface porosity (m^{-1})	28
Gas permeation rate @ 1.5 bar ($\frac{10^6\ cm^3\ (STP)}{cm^2\ cmHg\ s}$)	32032
Membrane porosity	0.834
LEPw (bar)	4.2
Membrane tortuosity	1.628

The presence of fingerlike macrovoids was confirmed by the SEM micrograph (Fig. 3), where the voids originate from the inner and outer surfaces and extend to the middle part of membrane cross-section. The voids near the outer surface are smaller and shorter due to the formation of the nascent skin layer at the outer surface while the fiber was travelling through the air gap. Furthermore, there is a thin spongelike layer in the middle of membrane cross section that can be ascribed to the slow phase inversion process in the middle of membrane cross-section where the penetration depth for the coagulant was the longest.

(a) **(b)**

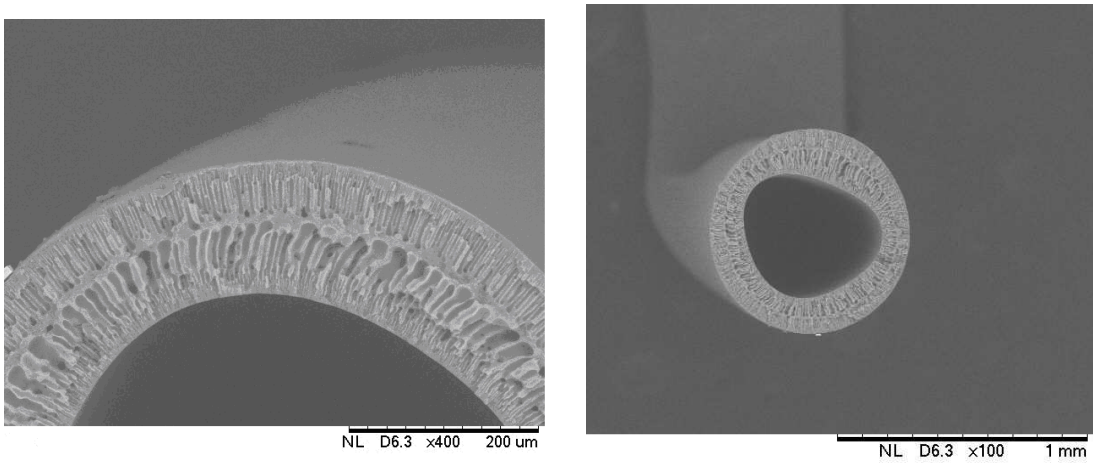

Fig. 3: SEM micrographs of fabricated membrane (a): partial cross-section, (b): full cross-section.

The experimental values obtained from the gas permeation tests are presented as helium gas permeance versus mean pressure together with the best fit linear line in Fig. 4. The surface properties of the membrane such as the pore size and the surface porosity were calculated using the method described in section 2.4.

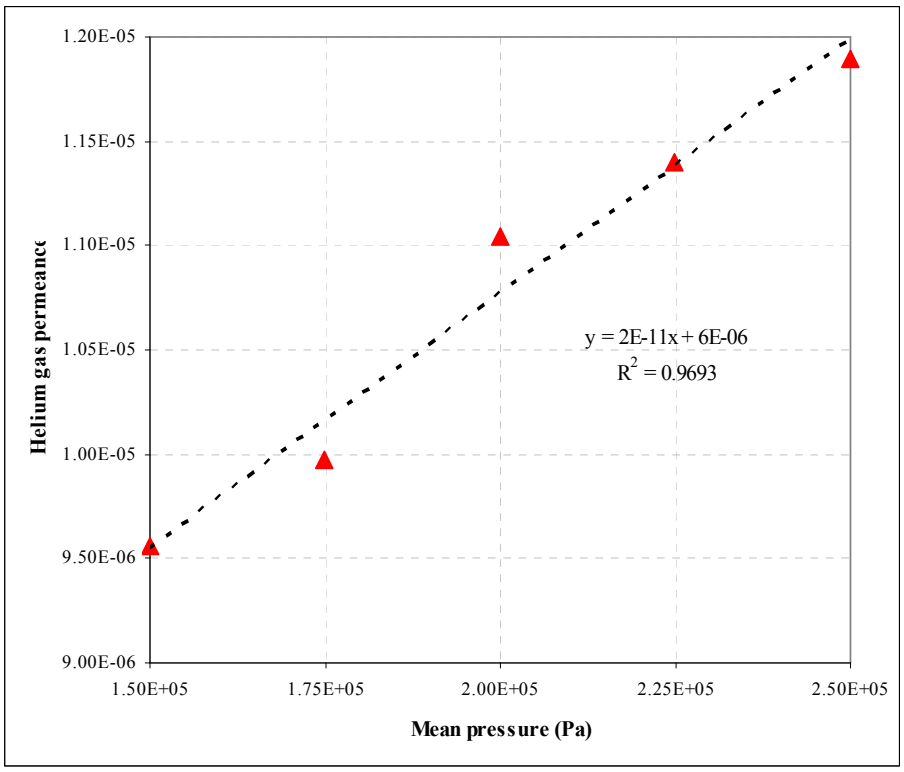

Fig. 4: The helium gas permanence versus mean pressure for fabricated membrane.

It was reported earlier that the structure of the skin layer strongly depends on the stability of the spinning solution [15]. The earlier study on the effect of nonsolvent additive to PEI spinning solution also showed that water as an additive made the spinning solution least stable, resulting in the membrane of high porosity and high gas permeance [16].

Blending water as a strong nonsolvent additive to PES solution reduces the thermodynamic stability of solution and enhances the surface porosity of membrane. In addition, the viscosity of PES/NMP/water solution is not significantly higher than the PES/NMP solution (the PES/NMP/water solution viscosity is 216.8 cp while the viscosity for the PES/NMP solution is 180 cp) even though the cloud point test results show a significant decrease in the stability of polymer solution (7.481 g water per 100 g solution for PES/NMP/water solution and 11.99 g water for PES/NMP solution). Therefore, the spinning solution used in this study has a low thermodynamic stability and a viscosity which enable to create a porous membrane, suitable for contactor applications.

The penetration of liquid into membrane pores reduces the vapor diffusion path length in the pore as reported elsewhere [17]. However, the penetration of liquid into membrane pores increases the heat transfer resistance as the liquid is stagnant in the pores. Furthermore, controlling the penetration depth in the membrane pores is not easy and complete filling the pores with liquid may contaminate the gas stream with liquid droplets. Therefore, penetration of liquid into membrane pores reduces the water flux by the latter effect.

The LEPw value is sufficiently high to prevent the pore wetting. It should be noted however that LEPw test was done at room temperature. LEPw may change significantly at high temperatures since the water surface tension and contact angle decrease with an increase in temperature.

3.2. Humidification test results

3.2.1. Effect of liquid velocity

Water flux and RH are plotted versus the liquid velocity in Figs. 5(a1,a2) and 5(b1,b2). When the liquid temperature is 30^{o}C, both flux and RH increase with an increase in liquid velocity until they level off. Similar results were reported earlier [5-7]. This is due to the decrease in the heat transfer resistance of the liquid boundary layer with an increase in liquid velocity, which leads to the reduction in temperature polarization. At the high liquid velocity, however, the heat transfer resistance of the liquid boundary layer no longer dominates the overall heat transfer resistance and, as a result, the flux and RH level off. Interestingly, when the liquid temperature is 60^{o}C, both flux and RH keep increasing with an increase in liquid velocity without leveling off. A plausible explanation is that the membrane heat transfer resistance decreases as the transfer of water vapor increases at the high liquid temperature, and the liquid phase heat transfer resistance keeps dominating even at the high liquid flow rate. Hence, the flux and RH do not level off.

a1

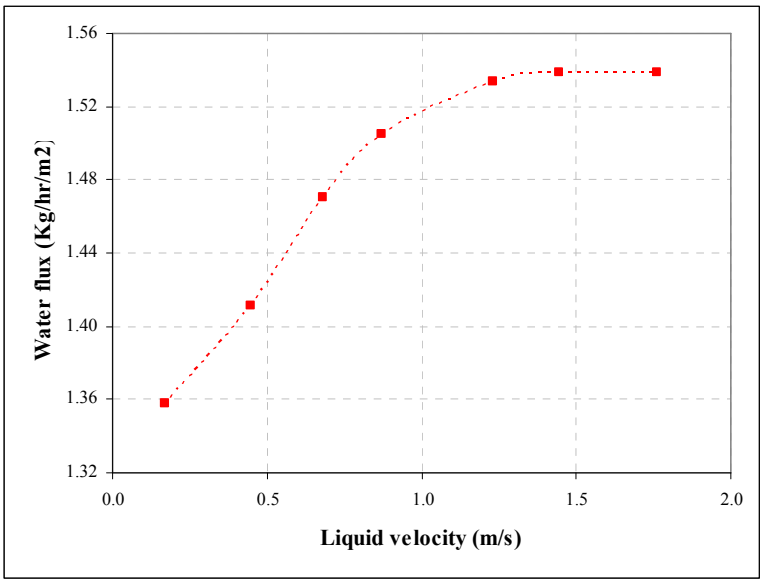

a2

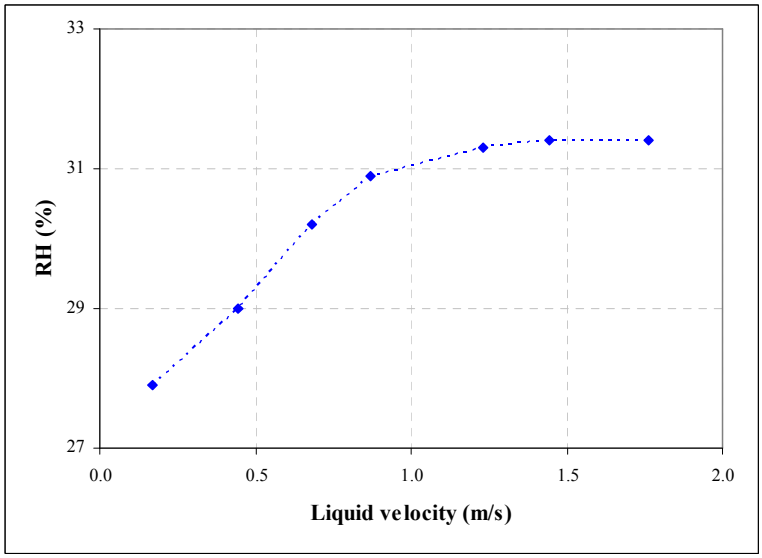

b1

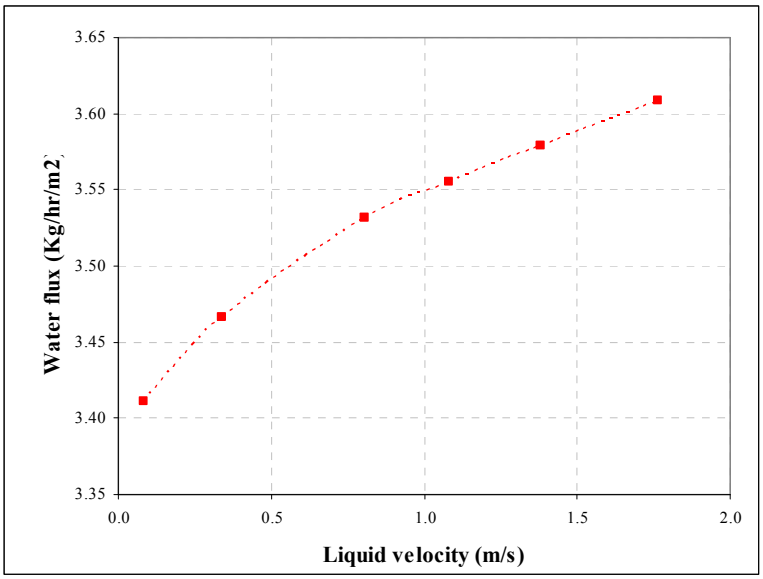

b2

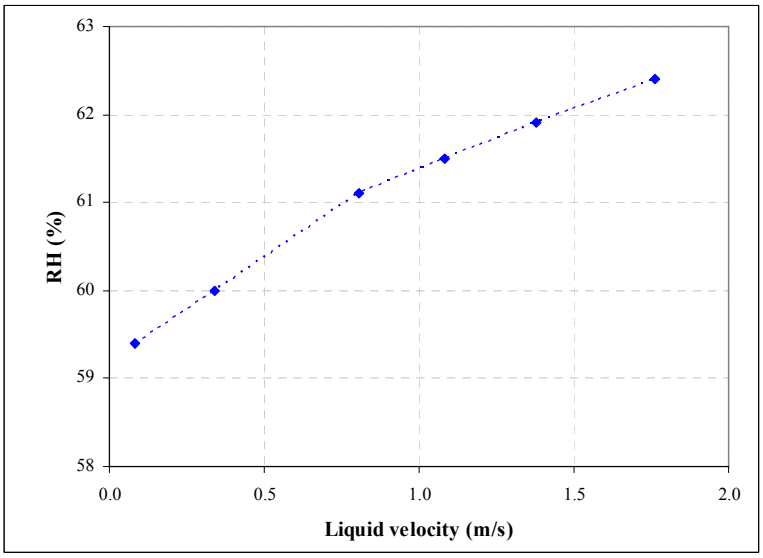

Fig. 5: The plot of water flux and relative humidity of the exit gas versus liquid velocity,

(a) T = 30 ^{o}C, P = 1 bar, Q_{gas} = 3 SLPM.

(b) T = 60 ^{o}C, P = 1 bar, Q_{gas} = 3 SLPM.

3.2.2. Effect of liquid temperature

The vapor pressure of liquids increases with temperature according to Antoine equation, so the water flux and RH of the exit gas increases with liquid temperature [5,6,18,19] as shown in Fig. 6(a,b).

(a)

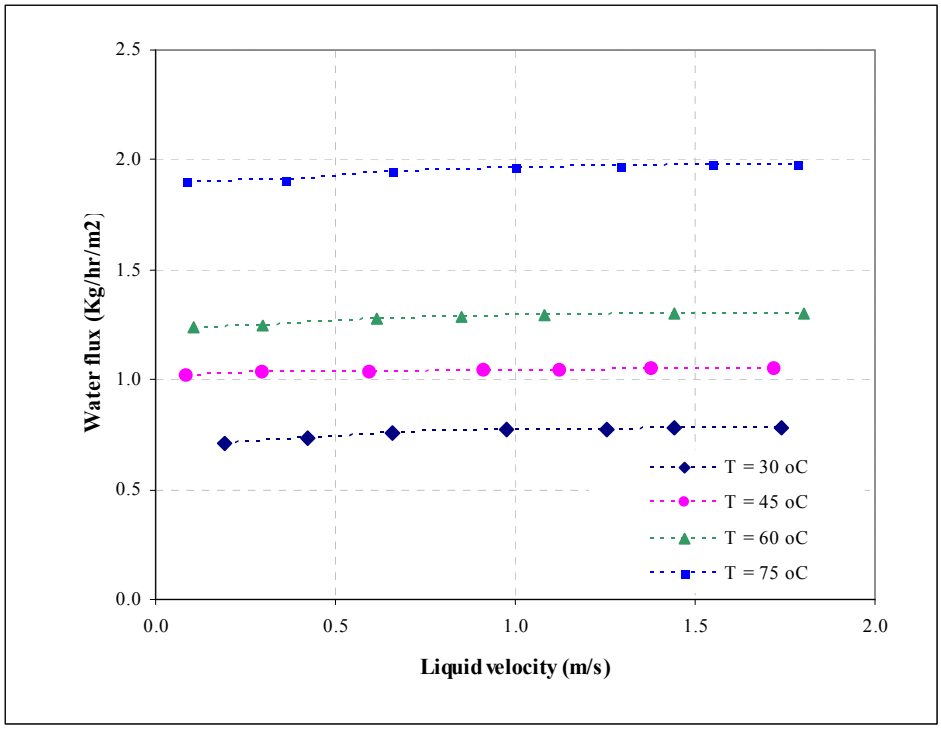

(b)

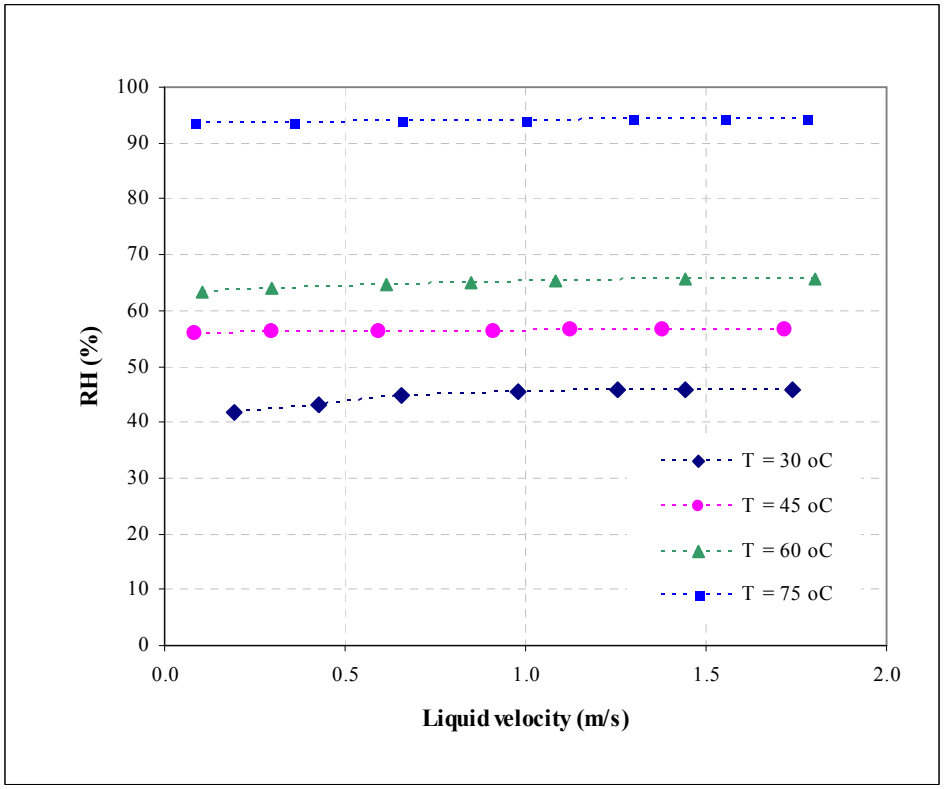

Fig. 6: The plot of (a) water flux and (b) relative humidity of the exit gas at different liquid temperatures; P = 1 bar, Q_{gas} = 1 SLPM.

According to Arrhenius equation (Eq. 11), water flux W (kg m^{-2} hr^{-1}) was plotted versus $1/T$ for the liquid velocities of 0.5, 1 and 1.5 m s^{-1}. Fig. 7 shows an example of V_{liquid} = 1 m s^{-1}, while similar linear relationships were obtained for the other liquid velocities with R^2 more than 0.97. Based on the plots, the average activation energy was 17.7 kJ mol^{-1}, which is much smaller than the heat of evaporation of water (44 kJ mol^{-1} at 25°C) due to the effects of the other factors such as the mass transfer coefficients.

$$W = W_0 \exp(\frac{-E}{RT}) \quad (11)$$

where W_0 is preexponential factor (kg m^{-2} hr^{-1}) and E is activation energy (J mol^{-1}).

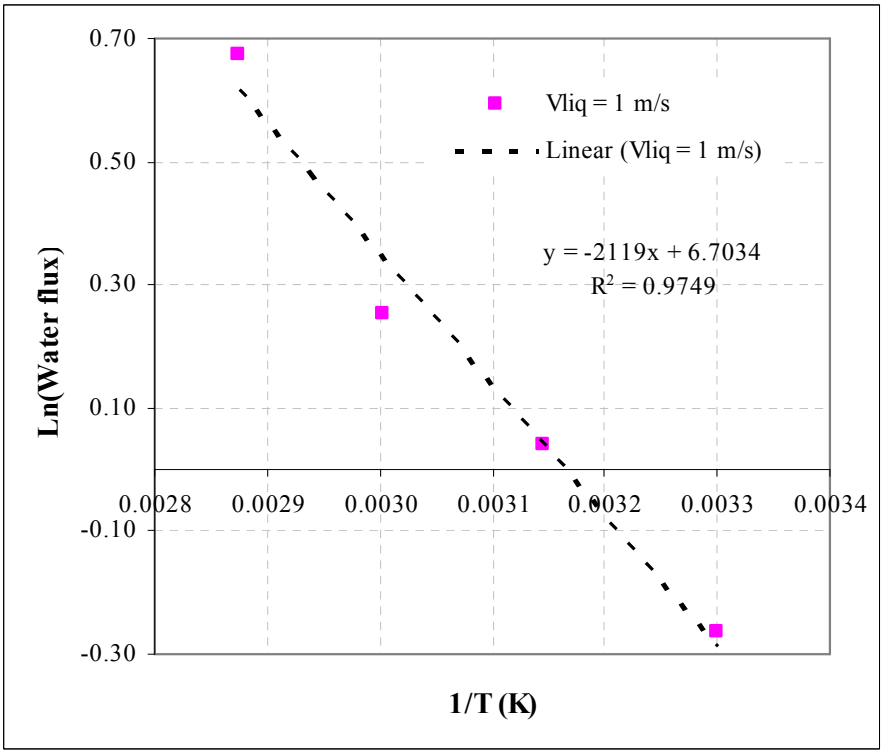

Fig. 7: The plot of Ln(water flux) versus T^1 for V_{liquid} = 1 m s^{-1}.

Furthermore, increasing liquid temperature improves the temperature gradient in liquid side of the contactor which enhances the heat transfer to the liquid on the membrane surface. In addition, heat is transferred from liquid phase to the gas stream by two mechanisms: 1- conduction through the membrane 2- through the sensible heat of transferred vapor. Higher water temperature enhances the heat transfer to gas phase by these two mechanisms and increases the absorption capacity of gas for vapor. In Fig. 8, the temperatures of exit gas versus liquid velocity at different liquid temperatures were presented.

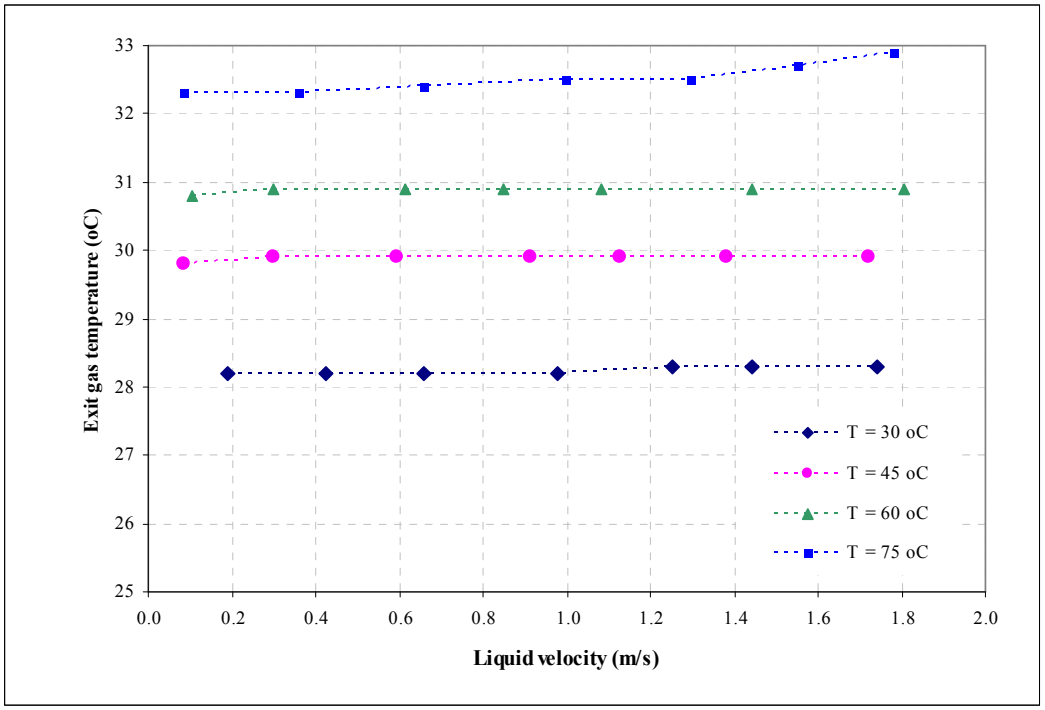

Fig. 8: The plot of exit gas temperature at different liquid temperatures; P = 1 bar, Q_{gas} = 3 SLPM.

3.2.3. Effect of pressure

In Figs. 9(a,b) and Figs. 10(a,b), the water flux and RH at two different pressures are shown. From both figures, water flux and RH decrease considerably with gas pressure, as also reported in [20]. This is because diffusivity of water vapor decreases in the gas boundary

layer as the gas pressure increases. Furthermore, the absorption capacity of gas for water vapor reduces with increasing the gas pressure.

(a)

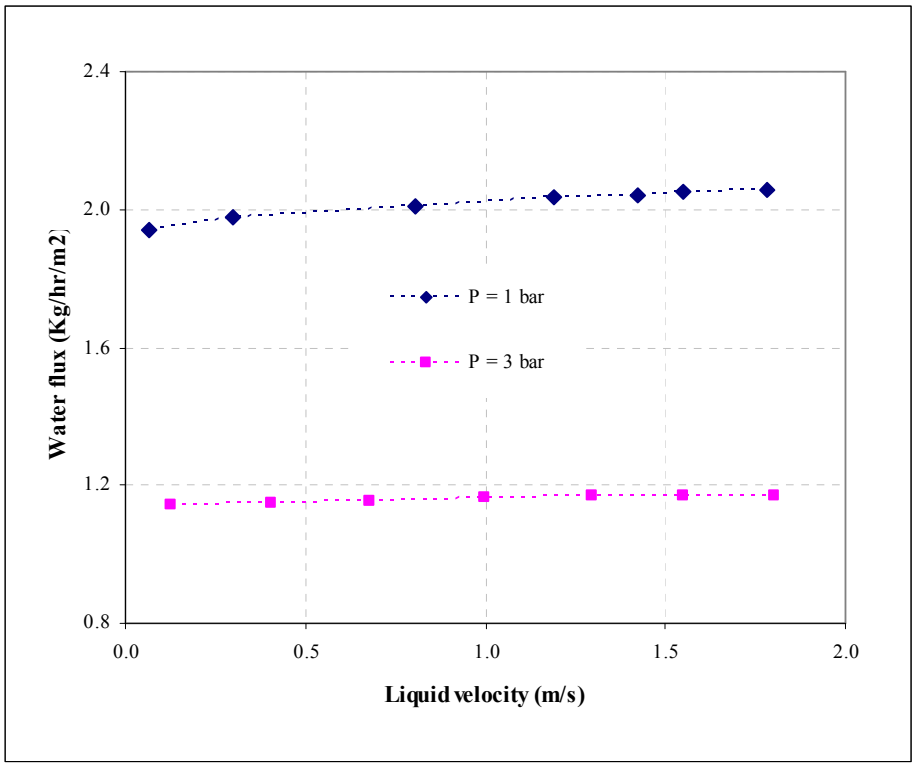

(b)

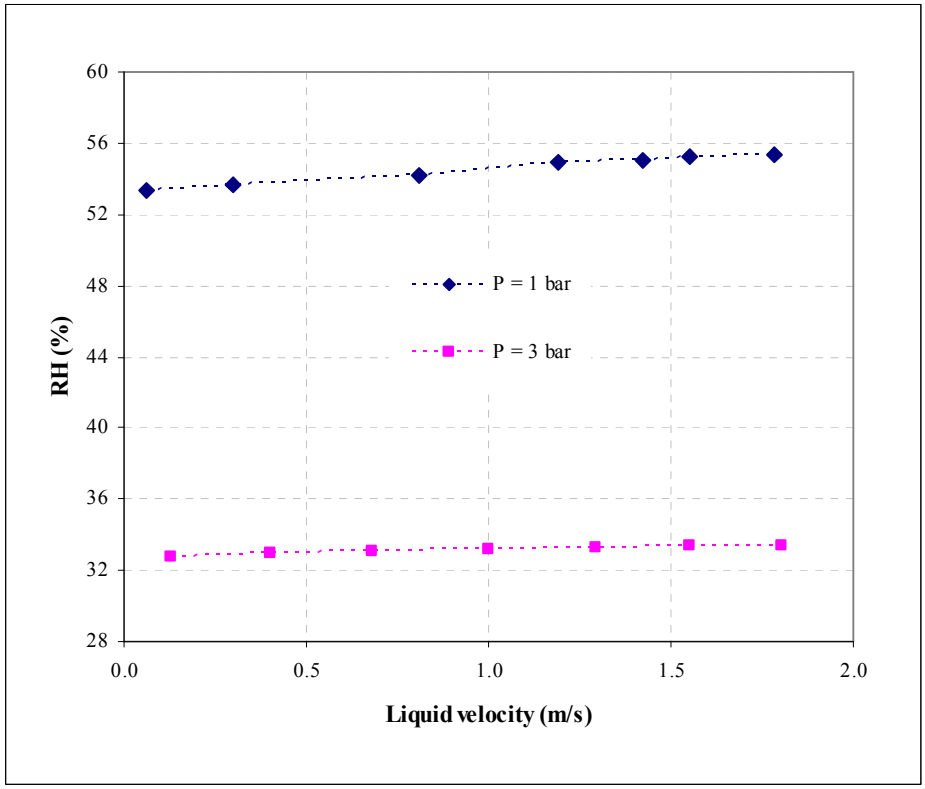

Fig. 9: The plot of (a) water flux and (b) relative humidity of the exit gas at different pressures; T = 45 ^{o}C, Q_{gas} = 2 SLPM.

(a)

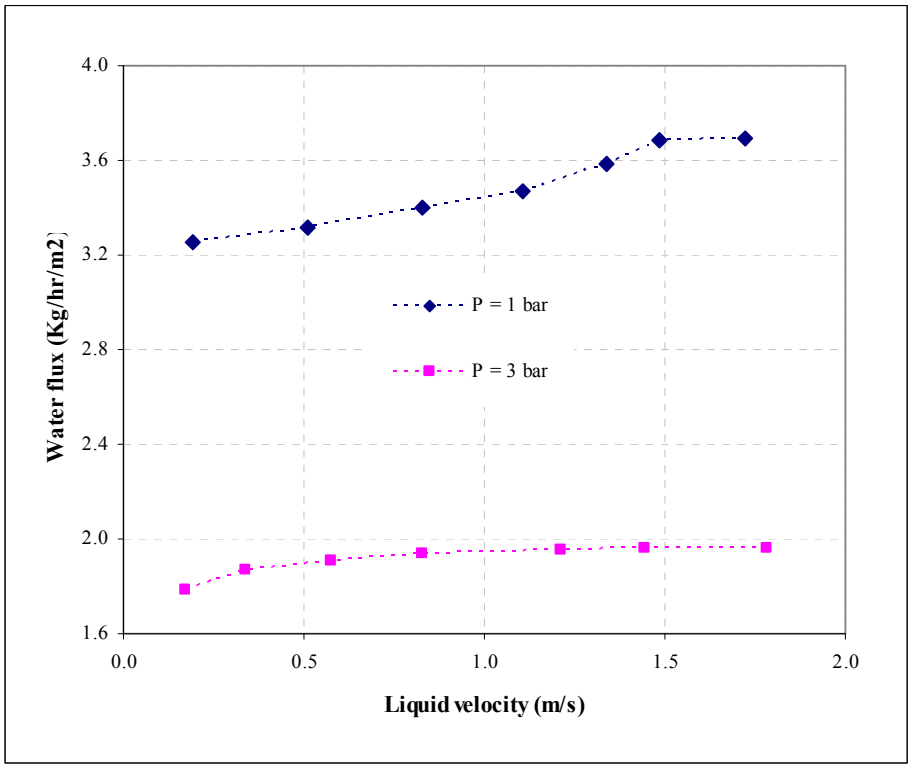

(b)

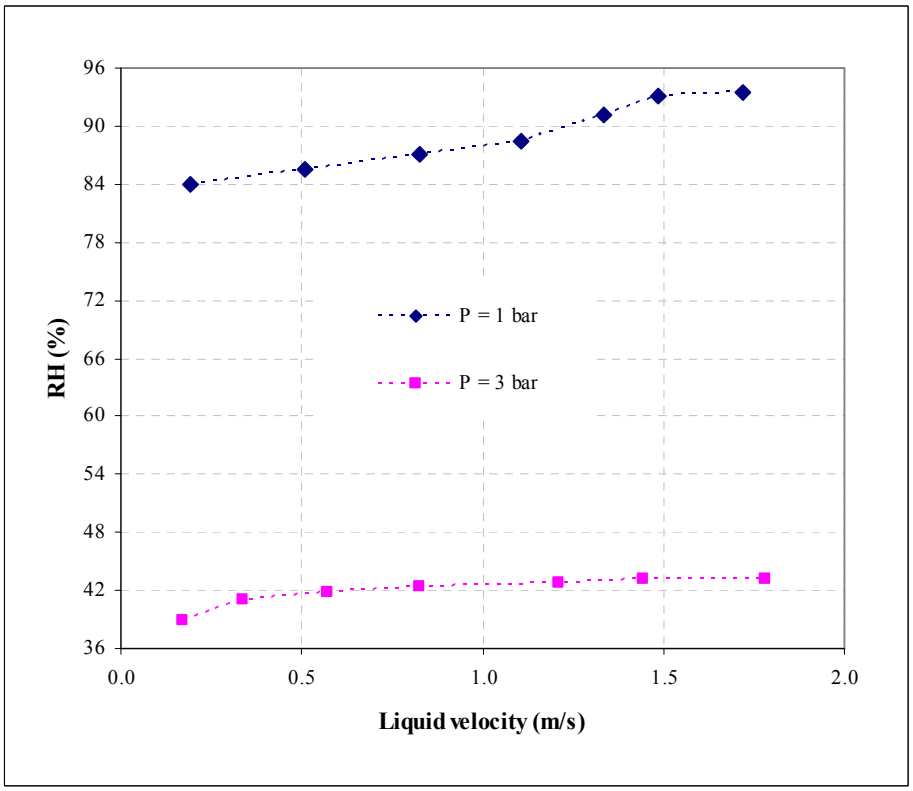

Fig. 10: The plot of (a) water flux and (b) relative humidity of the exit gas at different pressures; T = 75 ^{o}C, Q_{gas} = 2 SLPM.

3.2.4. Effect of gas flow rate

Figs. 11(a,b) show the effect of gas flow rate on the water flux and RH. The water flux increases with the gas flow rate, since the mass (and heat) transfer resistance decreases as the gas flow rate increases [7,18,21]. However, the vapor pressure of water in the exit gas decreases as the gas flow rate increases, therefore RH decreases [3,5,17,20].

(a)

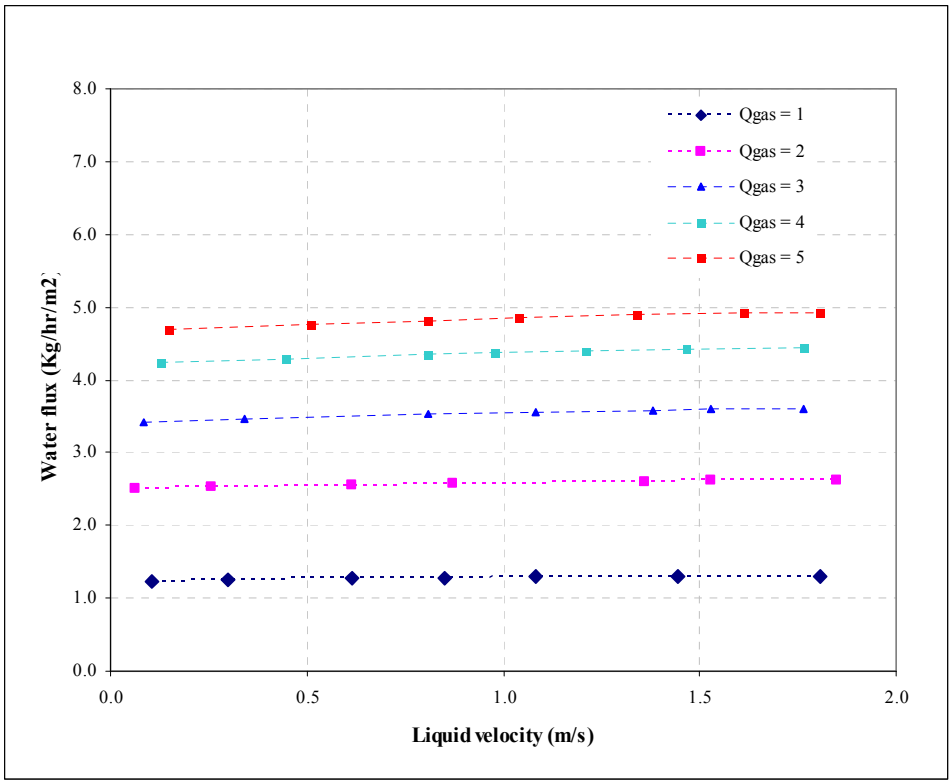

(b)

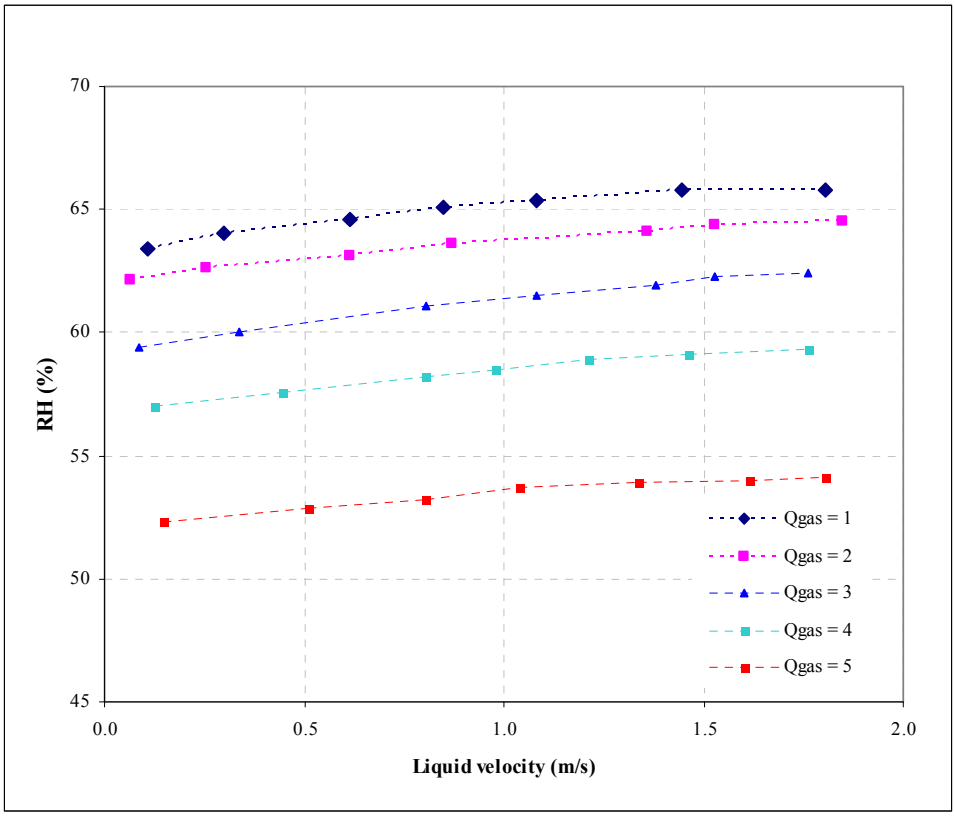

Fig. 11: The plot of (a) water flux and (b) relative humidity of the exit gas at different gas flow rates; T = 60 ^{o}C, P = 1 bar.

The results obtained in this study were compared with the results reported by other researchers. Chen et al. [18] used a commercial Nafion membrane based humidifier, Perma Pure®[1] model PH-60T-24SS and studied the effect of operating parameters. The humidifier comprises 60 Nafion membranes with a length of 610 mm and inner and outer diameter of 1.32 mm and 1.6 mm, respectively. Water flows in the shell side of humidifier while dry gas flows in the lumen side. The temperatures of air (T_{air}) and water (T_{liquid}) were kept constant at 27 ^{o}C and 19 ^{o}C, respectively, and the air flow rate (Q_{gas}) was 10 SLPM. Corresponding to these operational parameters, the water flux was 0.08 L m^{-2} h^{-1}. In this work, at T_{liquid} = 30 ^{o}C, gas pressure (P) = 1 bar and Q_{gas} = 5 SLPM, the water flux was 2.13 L m^{-2} h^{-1}, which is 2700% higher than Chen et al.'s result. As well, in Chen et al.'s work, corresponding to T_{air}

and Q_{gas} of 22 ^{o}C and 50 SLPM, respectively, and T_{liquid} = 40 ^{o}C, the water flux was 0.44 L m^{-2} h^{-1}, which is 380% lower than the value obtained in this work.

Kang et al. [21] used a commercial humidifier, Perma Pure 150-480-7PP, for their experiments. The humidifier contained 480 Nafion membranes with a length of 17.8 cm and inner and outer diameters of 0.71 mm and 0.76 mm, respectively. Water flows through the lumen side and gas flows through the shell side of the contactor. When T_{liquid} and T_{air} were 60 ^{o}C and 25 ^{o}C, respectively, and at Q_{gas} = 25 L min^{-1}, the water flux was 1.77 L m^{-2} h^{-1}. In this work, corresponding to T_{liquid} = 60 ^{o}C and Q_{gas} = 5 SLPM, water flux and is 4.93 L m^{-2} h^{-1} which is 180% higher than Kang et al.'s work.

Samimi et al. [17] fabricated porous PES and PS flat sheet membranes incorporating TiO_2 nanoparticles to increase the hydrophilicity of the membranes for gas humidification. The highest water flux was obtained by the membrane fabricated from the solution composed of 16 wt% PS and 0.1 wt% TiO_2 in DMF, which was 0.2125 L m^{-2} h^{-1} at T_{liquid} = 25 ^{o}C and Q_{gas} = 1 L min^{-1}. In this work, corresponding to the same operating conditions, the water flux was 0.78 L m^{-2} h^{-1}, which is 260% higher than Samimi et al.'s work. The significant difference in water flux is probably due to the lower wettability of PES hollow fiber membrane which prevents the penetration of liquid into membrane pores. Yang et al. [6] studied the effect of membrane pore size on the effectiveness of humidifier using PTFE and PVDF membranes. They showed that the effectiveness decreases as the pore size increases. Unlikely, Samimi et al. [17] reported that water penetration into membrane pores decreases the diffusion distance between liquid surface and gas stream and can enhance the performance of humidifier.

Table 5: Comparison of water flux of fabricated PES Membrane with in-house made and commercial membranes.

Polymer type	Membrane type	Fluid in lumen	Fluid in shell	Liquid temp. (^oC)	Gas temp. (^oC)	Liquid velocity (m s^{-1})	Gas flow rate (SLPM)	Water flux (L m^{-2} h^{-1})	Ref.
Nafion	HF	dry gas	water	40	22	NA	50	0.44	[18]
PES	HF	water	dry gas	30	room	1.8	5	2.13	this study
Nafion	HF	water	dry gas	60	25	NA	25	1.77	[21]
PES	HF	water	dry gas	60	room	1.81	5	4.93	this study
PS	flat sheet	-	-	25	NA	NA	1	0.21	[17]
PES	HF	water	dry gas	30	room	1.7	1	0.78	this study

HF: hollow fiber

NA: not available

4. Conclusions

PES hollow fibers were fabricated by the dry-wet spinning method with water as the nonsolvent additive to promote the phase inversion process. The hollow fibers were then characterized by the mean pore size, porosity and LEPw. The hollow fibers were further tested for gas humidification and the effects of various operating parameters on the water flux and relative humidity of exit gas were investigated. The conclusions are as follow:

1- The fabricated hollow fiber membrane has a high porosity and a large mean pore size due to the fast phase inversion process.

2- Finger-like macrovoids were formed in the membrane due to the fast intrusion of coagulant into membrane structure.

3- The membrane's LEPw is high enough for the long term operation of humidifier.

4- The water flux and relative humidity of exit gas increased with an increase in liquid flow rate.

5- The water flux and relative humidity of exit gas increased with the liquid temperature.

6- The water flux and relative humidity of exit gas decreased with an increase in gas pressure.

7- The water flux increased and the relative humidity of exit gas decreased with the gas flow rate.

8- The fabricated membrane showed higher water flux than any of in-house made and commercial humidifiers, e.g. at T_{liquid} = 30 ^{o}C, P = 1 bar and Q_{gas} = 5 SLPM, the water flux of PES membrane is 2700% higher than a commercial humidifier, Perma Pure®[1] model PH-60T-24SS.

Nomenclature

A_P	area of pores (m^2)	p_d	downstream pressure (Pa)
A_T	area of membrane (m^2)	R	universal gas constant (8.314 J mol^{-1} K^{-1})
L_P	effective pore length (m)	$r_{P,m}$	mean pore radius (m)
M	molecular weight (Kg mol^{-1})	T	absolute temperature (K)
P_K	gas permeance under Knudsen flow regime (mol m^{-2} Pa^{-1} s^{-1})	ξ	surface porosity
P_P	gas permeance under Poiseuille flow regime (mol m^{-2} Pa^{-1} s^{-1})	μ	viscosity (Pa. s)
$\overline{P}$	total gas permeance (mol m^{-2} Pa^{-1} s^{-1})	ε	membrane porosity
$\overline{p}$	mean pressure (Pa)	τ	membrane tortuosity
p_u	upstream pressure (Pa)		

References:

[1] G. Vasua, A.K. Tangirala, B. Viswanathan, K.S. Dhathathreyan, Continuous bubble humidification and control of relative humidity of H2 for a PEMFC system, Int. J. Hydrogen Energy 33 (2008) 4640-4648.

[2] A. Traverso, Humidification tower for humid air gas turbine cycles: experimental analysis, Energy 35 (2010) 894-901.

[3] S.K. Park, E.A. Cho, I.H. Oh, Characteristics of membrane humidifiers for polymer electrolyte membrane fuel cells, Korean J. Chem. Eng. 22(6) (2005) 877-881.

[4] J.R. Du, L. Liu, A. Chakma, X. Feng, Using poly(N,N-dimethylaminoethylmethacrylate)/polyacrylonitrile composite membranes for gas dehydration and humidification, Chem. Eng. Sci. 65 (2010) 4672-4681.

[5] K. Ramya, J. Sreenivas, K.S. Dhathathreyan, Study of a porous membrane humidification method in polymer electrolyte fuel cells, Int. J. Hydrogen Energy 36 (2011) 14866-14872.

[6] M. Yang, S.M. Huang, X. Yang, Experimental investigations of a quasi-counter flow parallel-plate membrane contactor used for air humidification, Energy Build. 80 (2014) 640–644.

[7] L.Z. Zhang, S.M. Huang, Coupled heat and mass transfer in a counter flow hollow fiber membrane module for air humidification, Int. J. Heat Mass Transfer 54 (2011) 1055-1063.

[8] M. Rezaei, A.F. Ismail, S.A. Hashemifard, Gh. Bakeri, T. Matsuura, Experimental study on the performance and long-term stability of PVDF/Montmorillonite hollow fiber mixed matrix membranes for CO_2 separation process, Int. J. Greenhouse Gas Control 26 (2014) 147-157.

[9] K. Li, Ceramic membranes for separation and reaction, John Wiley & Sons, 2007.

[10] Gh. Bakeri, A.F. Ismail, M. Rahimnejad, T. Matsuura, D. Rana, The effect of bore fluid type on the structure and performance of polyetherimide hollow fiber membrane in gas–liquid contacting processes, Sep. Purif. Technol. 98, 262-269.

[11] S. Srisurichan, R. Jiraratananon, A.G. Fane, Mass transfer mechanisms and transport resistances in direct contact membrane distillation process, J. Membr. Sci. 277 (2006) 186-194.

[12] W. Albrecht, Th. Weigel, M. Schossig-Tiedemann, K. Kneifel, K.V. Peinemann, D. Paul, Formation of hollow fiber membranes from poly(ether imide) at wet phase inversion using binary mixtures of solvents for the preparation of the dope, J. Membr. Sci. 192 (2001) 217-230.

[13] S.A. McKelvey, W.J. Koros, Phase separation, vitrification, and the manifestation of macrovoids in polymeric asymmetric membranes, J. Membr. Sci. 112 (1996) 29-39.

[14] A.J. Reuvers, C.A. Smolders, Formation of membranes by means of immersion precipitation: Part II. the mechanism of formation of membranes prepared from the system cellulose acetate-acetone-water, J. Membr. Sci. 34 (1987) 67-86.

[15] A. Mansourizadeh, A.R. Pouranfard, Microporous polyvinylidene fluoride hollow fiber membrane contactors for CO_2 stripping: Effect of PEG-400 in spinning dope, Chem. Eng. Res. Des. 92 (2014) 181-190.

[16] Gh. Bakeri, T. Matsuura, A.F. Ismail, The effect of phase inversion promoters on the structure and performance of polyetherimide hollow fiber membrane using in gas–liquid contacting process, J. Membr. Sci. 383 (2011) 159-169.

[17] A. Samimi, S.A. Mousavi, A. Moallemzadeh, R. Roostaazad, M. Hesampour, A. Pihlajamaki, M. Manttari, Preparation and characterization of PES and PSU membrane humidifiers, J. Membr. Sci. 383 (2011) 197– 205.

[18] D. Chen, W. Li, H. Peng, An experimental study and model validation of a membrane humidifier for PEM fuel cell humidification control, J. Power Sources 180 (2008) 461-467.

[19] J.R. Du, L. Liu, A. Chakma, X. Feng, Using poly(N,N-dimethylaminoethyl methacrylate)/polyacrylonitrile composite membranes for gas dehydration and humidification, Chem. Eng. Sci. 65 (2010) 4672-4681.

[20] D. Kadylak, W. Mérida, Experimental verification of a membrane humidifier model based on the effectiveness method, J. Power Sources 195 (2010) 3166-3175.

[21] S. Kang, K. Min, S. Yu, Two dimensional dynamic modeling of a shell-and-tube water-to-gas membrane humidifier for proton exchange membrane fuel cell, Int. J. Hydrogen Energy 35 (2010) 1727-1741.

Research highlights

- Porous PES hollow fiber membrane was fabricated with water used as a nonsolvent additive in the spinning solution.
- The membrane possessed large pores, high porosity and low wettability, which were the desirable properties for contactor application.
- The fabricated membrane was used in humidification process, where the effect of liquid and gas flow rates, liquid temperature and gas pressure on the water flux were studied.
- The membrane showed high performance compared to the commercial Nafion based membrane and porous in-house made membranes.